Indian Journal of Pure & Applied Physics
Vol. 59, January 2021, pp. 11-22

A Combined Experimental and first principle studies on $(ZnO)_{12}$ nanocluster

S Dheivamalar[a*] & K Bansura banu[a,b]

[a] PG & Research Department of Physics, Periyar E V R College (Autonomous), Tiruchirappalli-620 023, India

[b] PG & Research Department of Physics, Holy Cross College (Autonomous), Tiruchirappalli-620002, India

Received 24 December 2019; accepted 4 December 2020

We report the biogenic synthesis of ZnO nanoparticles using *Mangifera indica* aqueous extract and density functional theory/time-dependent density functional theory (DFT/TD-DFT) calculations on $Zn_{12}O_{12}$ nanocluster compared with various basis sets (B3LYP/6-31G, B3LYP/LANL2DZ, and B97D). The genesis of ZnO nanoparticles was achieved from the reduction of capping agent $ZnSo_4$. The properties of ZnO nanoparticles were signalized by UV, FTIR, FESEM-EDAX, and XRD analysis. The intense band at 380nm in the UV-Vis absorption spectrum results from the formation of ZnO nanoparticles. The structure of ZnO nanoparticles was anatomized by FESEM analysis and the presence of Zn was confirmed using EDAX. The frontier molecular orbital exploration has been investigated to govern the charge transfer characteristics of donor-acceptor moieties of the $Zn_{12}O_{12}$. The energy gap (Eg), binding energy (E_B), global reactivity descriptors, and the total dipole moment has also been investigated for $Zn_{12}O_{12}$. The total density of states (DOS) was analyzed to describe the orbital hybridization of $Zn_{12}O_{12}$. Mulliken atomic charge distribution, NBO analysis and molecular electrostatic potential (MEP) have also been studied. The first-order hyperpolarizability calculation proves that the $Zn_{12}O_{12}$ is a suitable candidate with the predominant nonlinear optical property. TD-DFT excited state analysis of $Zn_{12}O_{12}$ was completely consistent with the experimental data of the UV-Vis spectrum makes its application in solar cells.

Keywords: Nano cluster, $Zn_{12}O_{12,}$ Density of states, Density functional theory.

1 Introduction

Nano structured materials of II-VI and III-V semiconductors in modern sciences are currently of great interest due to their reduced dimensions and are majorly taking part in a dye-sensitized solar cell devices. The ZnO nanostructured materials are of greater importance owing to their nano morphology, nontoxicity, functionality, and biocompatibility[1-3]. The ZnO nanoparticles have gained the major attention of researchers due to their novel properties and probable applications in piezoelectric devices, UV absorbers, sensors, pharmaceuticals, and cosmetic industries[4,5]. The ZnO nanostructured material has an immense band gap which makes this material as the best semiconductor with the highest excitation binding energy in addition to low lasting threshold[6,7]. The developments of ZnO nano structured materials have been growing exponentially in the ended handful years, which were proven by numerous experimental and theoretical studies of ZnO related papers in the literature. The semiconductor ceramic compound ZnO exhibits good electrical conductivity and transmittance[8]. ZnO nanomaterial has pertinence in solar cells[9] gas sensors[10] piezoelectric materials[11] and electrodes[12]. The relative affluence of $(ZnO)_{11}$, $(ZnO)_{12}$ and $(ZnO)_{13}$ nanoclusters were majorly studied by Behran *et al.*[13]. The optoelectronic behavior of hexagonal structured ZnO nanocluster was analyzed by Malloci *et al.*[14]. The experimental observation of ZnO nanoparticles has been envisioned by Masuda *et al.*[15]. Among all these, fewer considerations have been adopted to correlate the experimental and theoretical observations of ZnO nanocluster. The preparation of ZnO nanomaerials was achieved through various synthesis techniques, namely sol-gel[16], hydrothermal[17], micro-wave assisted synthesis[18], micro-emulsion[19], chemical vapour deposition[20], vapour phase transport[21], homogeneous precipitation[22], direct precipitation[23], mechanochemical[24], spray pyrolysis[25] thermal decomposition[26] and radio frequency plasma[27]. Among all, the biogenic synthesis is the promising method to produce advanced functional nano particles. The biogenic synthesis is one the cleanest, biocompatible, non-toxic and eco-friendly methods through large-scale production[28]. *Mangifera Indica* well known as Mango that has been commonly used as a herb in ayurvedic medicine. The wide ranging survey of literature communicated that

*Corresponding author (E-mail: sitrulinsiragugal@gmail.com)

linear region of this plot gives direct energy band gap of 3.3 eV. This is also in good agreement to the DFT computed energy gap.

3.10 Surface Morphology by FESEM with EDAX analysis

The surface morphology and topography of ZnO nanoparticles was examined by Field emission scanning electron microscopy (FESEM) results. Figure 7 shows the FESEM image of synthesized ZnO nanoparticles. From the Fig. 6, we can find that the ZnO nanoparticles form a hexagon-like structure and this surface morphology is consistent with the theoretical optimal profile of $Zn_{12}O_{12}$ cluster. The mean grain size of ZnO was determined as 129 nm and it is in good agreement with the XRD results at 800 °C. The surface elements of ZnO were determined by energy-dispersive X-ray spectroscopy (EDAX). EDAX analysis confirms that the Zn and O atoms are present in the ZnO nanoparticle. The EDAX image was shown in Fig. 8. The amount of transition metal ions present in the ZnO nanoparticles are observed. In the ZnO nanoparticles, the composition of Zn and O atom was found to be Zn=48.86% and O=51.14%, respectively.

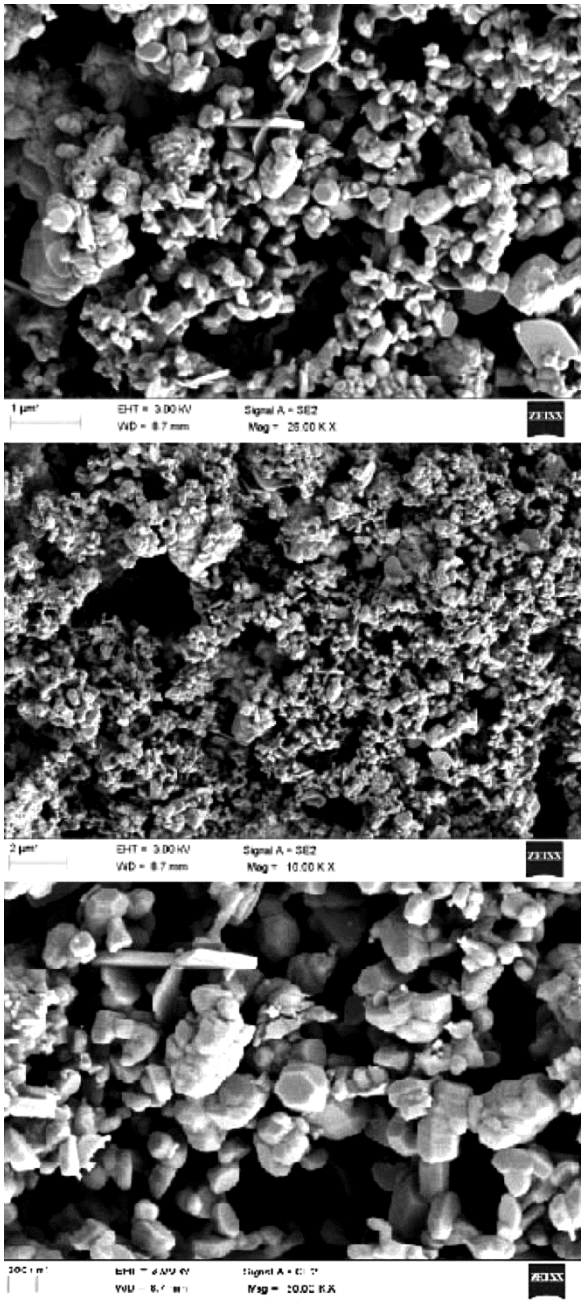

Fig. 7 — The FESEM image of green synthesized ZnO nanoparticles.

3.11 Vibrational assignments

The vibration frequencies are the unique parameter to explore the local minimum in structures. Transmittance is the principal features of Zn-O vibration[56]. The simulated IR spectrum of $Zn_{12}O_{12}$ shows the peaks at 430cm^{-1}, 451cm^{-1} and 547cm^{-1} have corresponded to the Zn-O stretching vibrations computed as B3LYP/6-31G level of geometry. In green synthesized ZnO nanoparticles, Zn-O is stretching was observed at 457 cm^{-1} and 545 cm^{-1}. The calculated peaks found at 451 cm^{-1} and 547cm^{-1} showing a better agreement with the experimental values. The synthesized ZnO nanoparticle showed approximate similar IR bands of $Zn_{12}O_{12}$ nanocluster that are seen in Fig. 9. Experimental and calculated vibrational frequencies in cm^{-1} for ZnO nanomaterial are listed in Table 7.

3.12 Natural Bond Orbital (NBO) analysis

The NBO calculated hybridizations are of great significance parameters for structure analysis. It was determined using the Gaussian 09 package at the B3LYP/6-31G (d,p) method. Natural Bond Orbital's are localized few-center orbital explain the Lewis-like

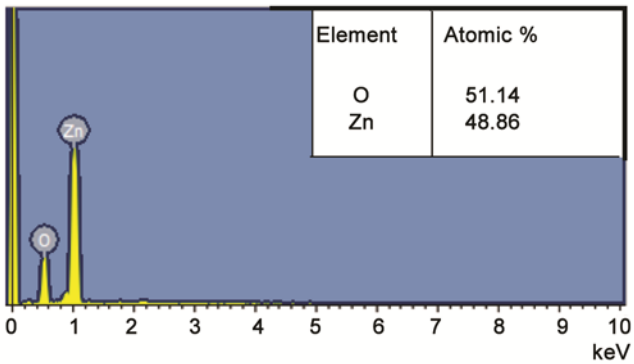

Fig. 8 — The EDAX spectra of ZnO nanoparticles.

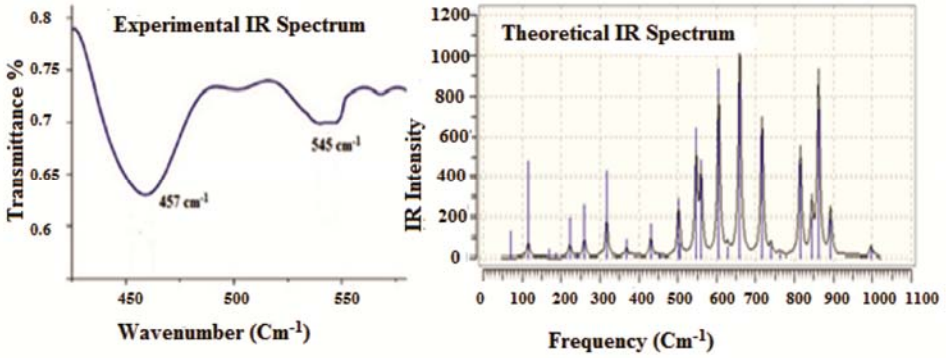

Fig. 9 — The simulated IR and experimental IR spectrum of ZnO nanoparticles

Table 7 — Experimental FT-IR and calculated vibrational frequencies in cm^{-1} for ZnO nanomaterial.

Experimental ZnO	Calculated B3LYP-$Zn_{12}O_{12}$	vibrational Assignment
457	451	Zn-O stretching
545	547	Zn-O stretching

molecular bonding pattern in the compact form of electron pairs.

NBOs are localized "maximum occupancy" orbital whose leading N/2 members (or N members in the open-shell case) and Lewis-like description of the total N-electron-density. Second-order perturbation theory indicates that all possible interactions are analyzed between "filled" (donor) Lewis-type NBOs and "empty" (acceptor) non-Lewis NBOs. Evaluation of NBO analysis helps to investigate the interaction between donor (i) level bonds donor-acceptor (j) level bands. The result of the interaction is a loss of occupancy from the concentration of electron NBO of the idealized Lewis structure into an empty non-Lewis orbital[57,58]. For each donor (i) and acceptor (j) the stabilization energy E(2) concerned with the delocalization i → j is as follows:

$$E(2) = \otimes Eij = qi(Fij)^2/(Ej-Ei)E(2) = \Delta Eij = qi(Fij)^2/(Ej-Ei) \quad \ldots (22)$$

Where qi is the donor orbital occupancy, Ei and Ej are the diagonal elements and Fij is the of diagonal NBO Fock matrix element. The NBO atomic charge transfer energy related to the electron donating from the π (Zn3-O4) to the acceptor antibonding π* (Zn3-O4) (Zn3-O24) orbital energies are 21.98, 15.29 kcal/mol results the strongest stabilization energy. Similarly, the interaction between the LP(1) O16, LP(3) O24 to the antibonding acceptor π* (Zn1-O16), (Zn3-O4) and their energies are 15.27, 12.18 Kcal/Mol. The large E(2) value exhibits the intensive interaction between electron-donors and electron-acceptors and the second order perturbation theory analysis of Fock matrix in NBO basis of $Zn_{12}O_{12}$ nanocluster are given in Table 8. Stabilization of the system was observed of the following strong

Table 8 — Second order perturbation theory analysis of Fock matrix in NBO basis of $Zn_{12}O_{12}$ nanocluster .

Donor (i)	Type	Acceptor (j)	Type	E(2)[a]	E(j)_E(i)[b]	F(i,j)[c]
Zn1-O16	π	Zn3-O4	π*	4.95	0.93	0.061
Zn1-O16	π	Zn3-O24	π*	1.13	0.72	0.026
Zn3-O4	π	Zn3-O16	π*	5.51	0.75	0.057
Zn3-O4	π	Zn3-O24	π*	5.55	0.76	0.058
Zn3-O16	π	Zn1-O16	π*	4.09	0.54	0.043
Zn3-O16	π	Zn3-O4	π*	21.98	0.98	0.131
Zn3-O16	π	Zn3-O24	π*	15.29	0.77	0.097
Zn3-O24	π	Zn3-O4	π*	4.9	0.94	0.061
Zn3-O24	π	Zn3-O16	π*	3.68	0.72	0.046
Zn3-O24	π	Zn3-O24	π*	1.41	0.73	0.029
LP(5) Zn1	n	Zn3-O16	π*	0.75	0.96	0.024
LP(5) Zn3	n	Zn3-O24	π*	0.62	0.94	0.022
LP(1) O4	n	Zn3-O4	π*	1.61	1.3	0.041
LP(1) O4	n	Zn3-O16	π*	2.2	1.08	0.044
LP(1) O4	n	Zn3-O24	π*	1.71	1.09	0.039
LP(2) O4	n	Zn3-O4	π*	5.51	1.39	0.078
LP(2) O4	n	Zn3-O16	π*	4.36	1.17	0.064
LP(2) O4	n	Zn3-O24	π*	3.7	1.19	0.059
LP(1) O16	n	Zn1-O16	π*	15.27	0.98	0.112
LP(1) O16	n	Zn3-O4	π*	3.37	1.41	0.062
LP(1) O16	n	Zn3-O16	π*	1.36	1.119	0.036
LP(1) O16	n	Zn3-O24	π*	3.28	1.21	0.057
LP(2) O16	n	Zn1-O16	π*	12.71	0.79	0.091
LP(2) O16	n	Zn3-O4	π*	4.16	1.22	0.064
LP(2) O16	n	Zn3-O16	π*	1.81	1	0.038
LP(2) O16	n	Zn3-O24	π*	1.06	1.02	0.032
LP(1) O24	n	Zn3-O4	π*	8.37	1.4	0.097
LP(1) O25	n	Zn3-O16	π*	4.29	1.18	0.064
LP(1) O26	n	Zn3-O24	π*	10.42	1.19	0.1
LP(3) O24	n	Zn3-O4	π*	12.18	0.92	0.097
LP(3) O24	n	Zn3-O16	π*	4.98	0.7	0.055
LP(3) O24	n	Zn3-O24	π*	7.23	0.71	0.066

intramolecular hyper conjugative interactions causing increased electron density (ED) and intramolecular charge transfer (ICT)[59].

4 Conclusion

The synthesis of ZnO nanoparticles using *Mangifera indica* through green chemistry approach with several advantages like economical, efficient, eco-friendly, energy efficient and cost-effectively provide a vast potential for their use in biomedical applications. We have reported the experimental study of ZnO nanoparticles and quantum chemical calculations of $Zn_{12}O_{12}$ through DFT/TD-DFT computations. The XRD predictions indicated that the green synthesized ZnO nanoparticles had a wurtzite structure. The optical band gap calculated from UV-Vis spectroscopy results ZnO nanoparticle absorb in the UV-Vis range. The FESEM image shows the spherical, cauliflower and irregular cluster morphologies. The structural parameters from XRD analysis was compatible with the frontier orbital analysis and optimized geometry of theoretical predictions. It is concluded that the lowest singlet excited state of the nanoparticle is mainly derived from the HOMO-LUMO (π- π^*) electronic transition. Information on the charge density distribution and site of chemical activity of the nanoparticle has been obtained by reactivity descriptors and MEP surface. Comparison of theoretical and experimental data exhibits good correlations confirming the reliability of the quantum chemical method to reveal the reactivity of the ZnO nanomaterial. The green synthesized ZnO nanoparticles provide healthier workplaces and communities leading to lessening waste and safer products. The green synthesis technique provides an easy and quick access to ZnO nanoparticles displaying greater interest for technological applications specifically for biomedical.

References

1 Naseem S M, Ahmed A & Tripathi P, *Optik*, 185 (2019) 599.
2 Mackowski S, Karczewski G, Wojtowicz, Qju X, Howe J Y, Mayer H M, Tuncer E & Parantharaman M P, *Appl Surf Sci*, 257 (2011) 4057.
3 Dheivamalar S & Bansura B K, *Orient J Chem*, 34 (2018) 5.
4 Duan J, Huang X & Wang E, *Mater Lett*, 60 (2006) 1918.
5 Aslanzadeh S, *J Mol Model*, 22 (2016) 160.
6 Abdulsattar M A, *J Mol Model*, 23 (2017) 125.
7 Sheng L, Gang L, Zhang W & Wang K, *Optik*, 184 (2019) 90.
8 Nakahara K, Takasu H, Fons P, Yamada A, Matsubara K, Hunger R & Niki S, *Appl Phys Lett*, 79 (2001) 4139.
9 Wang Z S, Huang C H, Huang Y Y, Hou Y J, Xie P H, Zhang B W & Cheng H M, *Chem Mater*, 13 (2001) 678.
10 Xu J Q, Pan Q Y, Shun Y A & Tian Z Z, *Sens Actuators B Chem*, 66 (2000) 277.
11 Sahu D R, Lin S Y & Huang J L, *Sol Energy Mater Sol Cells*, 91 (2007) 851.
12 Wang Z L & Song J H, *Science*, 14 (2006) 242.
13 Behran E C, Foehrweiser R K, Myers J R, French B F & Zandler M E, *Phys Rev A*, 49 (1994) R1543.
14 Malloci G, Chiodo L, Rubio A & Mattoni A, *J Phys Chem C*, 116 (2012) 8741.
15 Masuda Y, Yamagishi M, Seo W S & Koumoto K, *Crystal Growth Design*, 8 (2008) 1503.
16 Tokumoto M S, Pulcinelli S H, Santilli C V & Briois V, *J Phys Chem*, 107 (2003) 568.
17 Zhang H, Yang D, Ji Y, Ma X Y, Xu J & Que D L, *J Phys Chem B*, 18 (2004) 3955.
18 Hu X L, Zhu Y J & Wang SW, *Mater Chem Phys*, 88 (2004) 421.
19 Singhal M, Chhabra V, Kang P & Shah D O, *Mater Res Bull*, 32 (1997) 239.
20 Wu J J & Liu S C, *Adv Mater*, 14 (2002) 215.
21 Zhang Z, Yu H, Shao X & Han M, *Chem Eur J*, 11 (2005) 3149.
22 Kim J H, Choi W C, Kim H Y, Kang Y Y & Park K, *Powder Technol*, 153 (2005) 166.
23 Wang J M & Gao L, *Inorg Chem Commun*, 6 (2003) 877.
24 Tsuzuki T & McCormick P G, *Scripta Mater*, 44 (2001) 1731.
25 Okuyama K & Lenggoro I W, *Chem Eng Sci*, 58 (2003) 537.
26 Rataboul F, Nayral C, Casanove M J, Maisonnat A & Chaudret B, *J Organomet Chem*, 643 (2002) 307.
27 Sato T, Tanigaki T, Suzuki H, Saito Y, Kido O, Kimara Y & Kaito C, *J Cryst Growth*, 255 (2003) 313.
28 Yanrong L, Xueming Z, Yuna X, Junchen L, Shiting W & Hongze Z, *Optik*, 180 (2019) 151.
29 Sarsar V, Selwal K K & Selwal M K, *J Microbiology Biotechnol Res*, 3 (2013) 27.
30 Philip D, *Spectrochim Acta A; Mol Biomol Spectr*, 77 (2010) 807.
31 Kumar R S, Kumar S V, Ramaiah A, Agarwal H, Lakshmi T & Roopan S, *Enzym Microbial Technol*, 117 (2018) 91.
32 Dola S, Kumar V T & Subba R P S, *Prog Biomater*, 6 (2017) 57.
33 Frisch M J, Trucks G W, Schlegel H B, Scuseria G E, Robb M A, Cheeseman J R, Scalmani G, Barone V, Mennucci B, Peterson G A, Nakatsuji H, Caricato M, Li X, Hratchian H P, Izmaylov A F, Bloino J, Zheng G, Sonnenberg J L, Hada M, Ehara M, Toyota K, Fukuda R, Hasegawa J, Ishida M, Nakajima T, Honda Y, Kitao O, Nakai H, Vreven T, Montgomery J A, Jr, Peralta J E, Ogliaro F, Bearpark M, Heyd J J, Brothers E, Kudin K N, Staroverov V N, Kobayashi R, Normand J, Raghavachari K, Rendell A, Burant J C, IyengaSr S S, Tomasi J, Cossi M, Rega N, Millam M J, Klene M, Knox J E, Cross J B, Bakken V, Adamo C, Jaramillo J, Gomperts R, Stratmann R E, Yazyev O, Austin A J, Cammi R, Pomeli C, Ochterski J W, Martin R L, Morokuma K, Zakrzewski C G, Voth G A, Salvador P, Dannenberg J J, Dapprich S, Daniels A D, Farkas O, Foresman J B, Ortiz J V, Cioslowski J & Fox D J, Gaussian 09, Revision D.01, Gaussian, Inc Wallingford CT, (2009).
34 Lee C, Yang W & Parr R G, *Phys Rev B, 37* (1988) 785.

35 O'Boyle N M, Tenderholt A L & Langner K M, *J Comput Chem*, 9 (2008) 839.
36 Ochterski J W, Thermochemistry in Gaussian Inc, Pittsburgh, PA, (2000).
37 Ali S R & Khurshid A, *J Alloys Comp*, 678 (2016) 317.
38 Fatemeh F, Milad N & Sara S G, *Appl Surf Sci*, 366 (2016) 545.
39 Birajdar S D, Khirade P P, Bhagwat V, Humbe A V & Jadhav K, *J Alloys Compd*, 683 (2016) 513.
40 Seetawan U, Jugsujinda S, Seetawan T, Ratchasin A, Euvananont C, Junin C, Thanachayanont C & Chainaronk P, *Mater Sci Appl*, 2 (2011) 1302.
41 Wang Z L, *Mater Today*, 7 (2004) 26.
42 Hossain M F, Zhang Z H & Takahashi T, *Nano-Micro Lett*, 2 (2010) 53.
43 Noh Y J, Na S I & Kim S S, *Sol Energ Mat Sol Cells*, 117 (2013) 139.
44 Bacaksiz E, Aksu S, Yılmaz S, Parlak M & Altunbas M, *Thin Solid Films*, 518 (2010) 4076.
45 Yilmaz S, Bacaksiz E, McGlynn E, Polat I & Qzcan S, *Thin Solid Films*, 520 (2012) 5172.
46 Maniv S & Zangvil A, *J Appl Phys*, 47 (1978) 2787.
47 Wang X S, Wu Z C, Webb J F & Liu Z G, *Appl Phys A*, 77 (2003) 561.
48 Warren B E, X-ray diffraction, Dover, New-York (1990) 253.
49 Aksoy S, Caglar Y, Ilican S & Caglar M, *Adv Control Chem Eng Civ Eng Mech Eng*, (2010) 227.
50 Dheivamalar S & Bansura B K, *Indian J Pure Appl Phys*, 57 (2019) 713.
51 Koopmans T, *Physica*, 1 (1933) 104.
52 Yadav P S & Pandey D K, *Appl Nanosci*, 2 (2012) 351.
53 Ali S R & Khurshid A, *Thin Solid Films*, 612 (2016) 179.
54 Dheivamalar S & Bansura B K, *Heliyon*, 5 (2019) e02903.
55 Gaussview 4.1.2, Gaussian Inc, Wallingford, CT, (2004).
56 Fogarasi G, Zhov X, Taylor P W & Pulay P, *J Am Chem Soc*, 114 (1992) 8191.
57 Agarwal D C, *Nucl Instrum Methods Phys Res*, 244 (2006) 136.
58 Glendening E D, Reed A E, Carpenter J E & Weinhold F, NBO Version 3.1, TCI, University of Wisconsin: Madison, (1998).
59 Reed A E, Curtiss L A & Weinhold F, *Chem Rev*, 88 (1988) 899.